International Journal of Nanoelectronics and Materials
IJNeaM
ISSN 198-5761 | E-ISSN 2232-1535

Molecular-Imprinting Assisted Polydopamine-Aptasensor On Carbon and Gold Nanomaterials Construct for The Haemophilia B Biomarker Detection

Hemavathi Krishnan[a], Subash C.B. Gopinath[a,b,c,*], Tijjani Adam[d], Makram A. Fakhri[e], Evan T. Salim[f] and Narendra Patil[g]

[a]Institute of Nano Electronic Engineering, Universiti Malaysia Perlis (UniMAP), 01000 Kangar, Perlis, Malaysia.
[b]Faculty of Chemical Engineering & Technology, Universiti Malaysia Perlis (UniMAP), 02600 Arau, Perlis, Malaysia.
[c]Center for Global Health Research, Saveetha Medical College & Hospital, Saveetha Institute of Medical and Technical Sciences (SIMATS), Thandalam, Chennai – 602 105, Tamil Nadu, India.
[d]Faculty of Electronic Engineering & Technology, Universiti Malaysia Perlis (UniMAP), Arau 02600, Perlis, Malaysia.
[e]Laser and Optoelectronics Engineering. Department, University of Technology-Iraq, Baghdad, Iraq.
[f]Applied Science Department, University of Technology-Iraq, Baghdad, Iraq.
[g]Department of Pharmacology, Dr. A.P.J. Abdul Kalam University, Indore, India.
**Corresponding author. Tel.: +6011-10472006; e-mail: subash@unimap.edu.my*

ABSTRACT

The study presents a comprehensive approach for enhancing the performance of a spiral micro-interdigitated electrode (spiral-μIDE) sensor for the detection of FIX protein. Electropolymerization using dopamine resulted in a molecular-imprinted polymer (polyDOP-μIDE-MIP) layer, which encapsulated the aptamer-FIX complex and was later leached to create cavities. Cyclic and linear-sweep voltammetry techniques were utilized for the MIP development and rebinding assessment. Linear sweep voltammetry demonstrated a linear relationship between FIX concentration and peak current reduction, with a limit of detection (LOD) of 0.250 picomolar. The sensor's sensitivity was determined as 2.613E-10 $A.fM^{-1}.\mu m^{-2}$. This work highlights the importance of nanomaterials integration, and electropolymerization in improving sensor performance. The integration of carbon and gold nanomaterials and the use of molecular imprinting contribute to the sensor's enhanced sensitivity and selective detection of FIX protein.

Keywords: *Aptasensor, molecularly imprinted polymer, nanomaterials, protein-MIP, polydopamine*

1. INTRODUCTION

Rapid diagnosis of any disease is the primary solution to provide timely treatment. Haemophilia B is a rare bleeding disorder where a person lacks blood clotting factor IX protein. This disease is commonly undiagnosed, and some patients are facing unexpected mortality when the disease is not diagnosed at the early stage [1]. The regular treatment for them is blood transfusion or injection of plasma-derived clotting factor IX protein concentrates [2]. For this, a precise protein quantification method is required. Existing protein quantification assays such as enzyme-linked immunosorbent assay, and Lowry protein assay are laborious, time-consuming, and costly to quantify the protein level in a patient. The present study developed a molecular-imprinting based protein detection microsensor to quantify the clotting factor IX protein.

The molecular imprinting process is widely acknowledged as a highly effective approach for fabricating three-dimensional polymer matrices through the incorporation of a template molecule into a solution containing dissolved monomers and cross-linkers. Once the polymerization process is complete, the template is then extracted, resulting in the formation of perpetual cavities. These cavities possess the capability to rebind with the template molecules [3], [4]. MIP is highly stable and durable that is ideal for analytical requirements. The last three decades have seen major scientific efforts put into the development of MIPs for protein molecules, owing to their high selectivity and stability. Although MIP has been applied in various methods such as biosensor, drug delivery, and, chromatographic separation, positive results have been seen as recognition components in electrochemical sensors. However, MIP based electrochemical sensors required improved method to the existing method in terms of mass transfer rate and adsorption capacity [5]. Because of these issues, scientists have been exploring the potential of high-surface-area materials like nanomaterials conjugates [6].

Among the emerging nanomaterials, carbon and gold nanoparticles duos have shown remarkable potentials in MIP biosensor considering the selectivity, sensitivity, and imprinting capacity [7]. Carbon nanoparticles, such as carbon nanotubes and graphene derivatives, possess remarkable electrical, thermal, and mechanical properties. Adding these nanomaterials to MIP-based biosensors may increase their conductivity and hence their ability to transduce signals. Additionally, they also provide substantial surface areas for improved template immobilisation, increasing the binding capacity of the sensor. The sensitivity of the sensor can be improved by adding gold nanoparticles (AuNPs), which have their own set of distinctive features [8], [9]. The coordinated assembly of AuNPs within imprinted polymers enables more imprints

in the polymer that results is the high binding capacity of produced MIP as well as enhanced signal transduction [10]. Carbon and gold nanoparticles are incorporated into MIP matrices through a variety of techniques. Some examples include template-assisted techniques, layer-by-layer assembly, co-polymerization, and electrochemical deposition. Well-defined hierarchical structures may also be constructed via integration methods like electrostatic assembly and covalent bonding. This technique involves functionalizing carbon nanoparticles with linker molecules, followed by the attachment of gold nanoparticles. Thus, the present study encompasses the nanomaterial integration on a 50 µm gapped spiral interdigitated electrode (spiral-µIDE) using dopamine as the functional monomer.

2. MATERIALS AND METHODS

The surface characterization was performed by high power microscope (HPM), 3D-nanoprofilometry (Hawk 3D Optical-Surface Profiler, South Korea) to authenticate the electrode gap size and uniform layer during the MIP fabrication process. 2'-fluoro modified anticoagulant aptamer was synthesized commercially. Potassium hydroxide (KOH), (3-Aminopropyl) triethoxysilane (APTES), dopamine (DOP), potassium chloride (KCl), human plasma derived Factor IX (FIX), carbon and gold nanomaterials were bought from Sigma Aldrich (Missouri, USA). The RNA aptamer used in this study was obtained commercially with thiol (-SH) end modification for the sequence "5'AUG GGG ACU AUA CCG CGU AAU GCU GCC UCC CCA U-[(A)24] 3`".

2.1. Spiral-µIDE Surface Enrichment with Carbon and Gold Nanomaterials

Initially, the spiral-µIDE was treated with 1 M KOH to form more hydroxyl groups on the sensing region. The conductivity of the sensor was then enhanced by hierarchically stacking carbon and gold nanomaterial conjugates. For that, at first, APTES linker was used to create amine functional groups in carbon nanomaterial. Next, the gold nanomaterials are ionically reacted with by the amine from APTES modified carbon nanomaterials. Each nanomaterial was dispersed to the sensing area and incubated for 2 hours at room temperature. A 10-fold increase in washing solvent volume was used between each surface modification.

The thiol-functionalized aptamer was subjected to an activation procedure at 95 °C for 5 min. Then, 2 µM of FIX protein was added to a solution of 2 µM activated aptamer in phosphate-buffered saline (PBS) solution with a pH of 7.4 and a concentration of 10 mM, and the mixture was treated for an hour at room temperature. The aptamer-FIX complex was then carefully spread across the surface of the spiral-µIDE in a volume of 10 µL. The terminal thiolated aptamer immediately coupled with gold nanomaterials through the oligo-S interaction with gold nanomaterial, which was facilitated by the formation of strong Au-S bonds. In the subsequent step, the electrode was treated for 30 min with 2 µM FIX in order to saturate any unbound aptamers. The Apta-FIX-IDE electrode was subjected to a comprehensive cleansing procedure with PBS buffer and distilled water. The Apta-FIX-µIDE was immersed in a solution containing 10 mM PBS containing 5 mM DOP and 10 mM KCl to carry out the molecular imprinting procedure.

2.2. MIP Fabrication and Detection by Cyclic and Linear-sweep Voltammetry

An Autolab potentiostat/galvanostat (PGSTAT204, Metrohm Autolab; https://www.metrohm.com/en) was used to conduct cyclic voltammetry (CV) and linear sweep voltammetry. NOVA 2.0 software was used to control the potentiostat instrument and modify the experimental parameters. All tests were performed with three electrodes mounted in a three-electrode configuration with a reference electrode of Ag/AgCl and a nanoparticle modified spiral-IDE, which has a geometrical surface area of 19.635 μm^2 [11]. In 0.1 M phosphate buffer containing 5.0 mM $K3[Fe(CN)6]/ K4[Fe(CN)6]$ (1:1), electrochemical measurements were carried out at potentials between -0.3 V and 1.2 V with 5.0 mV as the signal amplitude and 0.2 V as the bias potential. All CVs plots were obtained in the presence of 10 mL of 0. 1 M phosphate buffer (pH = 7.0) at scan rate of 0.02 V/s.

A molecular-imprinted polymer (polyDOP-µIDE-MIP) was created by electropolymerizing the surrounding FIX protein with dopamine using potential cyclic voltammetry (CV). The CV was conducted over a potential range of -1.5 V to 1.5 V, using a scan rate of 20 mV/s. The supporting electrolyte used was 5 mM KCl, as shown in Figure 1. The polymerized electrodes were immersed in a PBS buffer solution containing acetic acid and SDS (w/v 5%) to detach the protein that eventually forms specific cavities in the polymer matrix. Linear sweep voltammetry was used in experiments to test the sensitivity and sensing capabilities of FIX on polyDOP-IDE-MIP or that a range of 5 fM to 8 pM pure FIX solutions were diluted into seven concentrations. The rebinding assay commenced with the 10 µL of lowest concentration, 5 fM onto the polyDOP-µIDE-MIP. Following a 10-min incubation period, the sensor surface was subjected to a thorough washing using a 10-fold volume of PBS solution. Subsequently, the linear sweep voltammetry (LSV) technique was employed to measure the desired parameters. Similar method was used for further concentrations.

3. RESULTS AND DISCUSSION

The protein-imprinted polymer sensor was constructed using DOP as the functional monomer. The spiral-µIDE, treated with KOH, was subjected to functionalization with carbon and gold nanomaterial conjugates in a hierarchical manner, with the aim of enhancing the conductivity of the sensor. Then, a solution containing the aptamer-FIX complex was applied onto the functionalized surface, resulting in the formation of covalent bonds between the aptamer and gold nanomaterial through thiol-SH bonding. The use of covalent bonding in biosensor fabrication is highly efficient due to the ease of modifying functional groups in both biomolecules and fabrication matrices. For example, the aptamer end is commonly modified with thiol

or amine functional groups and a covalent linker modification on the biosensor surface [12], [13]. Following that, the adjacent FIX protein was subjected to electropolymerization using DOP through the utilization of potential cyclic voltammetry (CV), resulting in the formation of a molecular-imprinted polymer referred to as polyDOP-μIDE-MIP. The process of DOP oxidation results in the formation of polydopamine (polyDOP) layers that encapsulate the aptamer-FIX complex that is bound to it. Following the process of polymerization, the FIX protein molecules that were entrapped were subsequently removed through a mild chemical leaching technique employing a solution of 5% SDS/Acetic acid in distilled water [14]. The study conducted by [15] reveals that the interaction between the aptamer and FIX protein primarily involves electrostatic forces and weak hydrogen bonds. This solution effectively disrupts the weak hydrogen bonds between the aptamer and FIX proteins. The formation of cavities develops eventually by a template leaching process that carries similarities to the shape and physiochemical memory of the FIX protein. Overall MIP development procedure is illustrated in Figure 1.

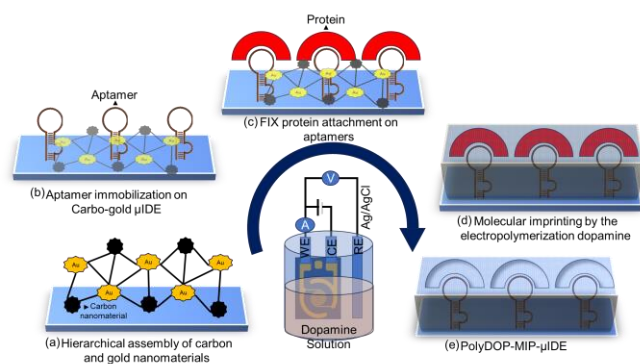

Figure 1. Schematic illustration of spiral-μIDE sensor surface enrichment with nanomaterials and MIP development for FIX protein template. (a) Surface functionalization of carbon and gold nanomaterials. (b) Aptamer immobilization. (c) FIX protein attachment. (d) Poly-dopamine polymer formation. (e)PolyDOP-MIP-μIDE sensor after FIX protein removal from the polymer matrix.

3.1. Nanomaterials Integration and Surface Characterization

Surface characterization was carried out to verify the sensor's edges and variances in finger and gap widths compared to the intended dimension. In addition, surface characterization was conducted to verify the attachment of nanomaterials. First, High performance microscopy was used to check the bare spiral-IDE for the impurities sensor's surface and damage-free electrodes (Figure 2a-b). As depicted in Figure 2c, the electrode thickness and surface were analyzed using a 3D-nanoprofiler. The height difference from SiO_2 surface to Al electrode was 70 μm. The smooth and clear surfaces of each layer confirm that the device is free of impurities, indicating that the sensor was clean prior to any surface functionalization. However, in Figure 2d, a coarse-grained surface is observed on the nanomaterials modified sensor. The hue variation for each layer highlights the silicon surface and the Al electrode surface (Figure 2e). The silicon surface is represented by blue, and the aluminium electrode by the orange colour. After nanomaterials modification, coarse particles were observed at 10000 magnifications after MIP fabrication (Figure 2f). The majority of the sensor's surface colour changed to a pale green, indicating a height increase due to the hierarchical nanomaterial arrangement. The thickness of nanomaterials was observed to be ~8.5 μm.

The reproducibility graph of the bare device for each surface modification is depicted in Figure 2g. Each surface modification was measured using a Picoammeter (Keithley 6487) as the voltage source set to 0 V to 2 V in order to observe the dielectric variations at the electrode surface for the supplied voltage. The maximal values of current for KOH, carbon-gold conjugates, and the aptamer-FIX complex were 4.7E-7, 3.9E-6, and 1.4E-6 A, respectively. Based on the present responses, the relative standard deviation (RSD) was calculated to be 3.13 %, which shows that the sensor gives good reproducibility.

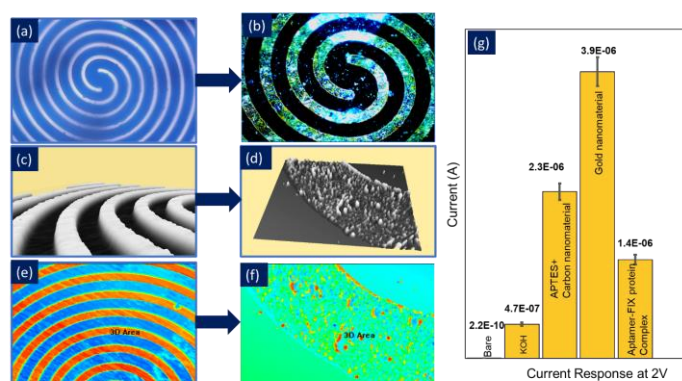

Figure 2. Surface characterization of bare and nanomaterials modified spiral-μIDE. Surface analysis by high-performance microscopy (a-b) and 3D nanoprofiler (e-f). The reproducibility plot of each modification is shown in bar diagram (g).

3.2. FIX Protein Imprinting by Electropolymerization

Any transducer surface can integrate MIPs using electropolymerization approach. The possibility of imprinting polymerization of dopamine, and the subsequent development of biosensors based on this material, was confirmed in experiments by [16]. With a similar approach, the current study performed electropolymerization using dopamine as the monomer solution. Dopamine's electrochemical oxidation has been studied [17], [18]. The electrochemical pathway for DOP entails the oxidation of dopamine, which results in the formation of dopaminequinone (DAQ). The subsequent cycle consists of the intramolecular cyclization of DAQ to the more easily oxidizable leucodopaminechrome (LDAC). LDAC is subsequently oxidised to dopaminechrome (DAC). On the electrode surface, DAC can endure additional polymerization reactions to produce polyDOP layers.

Table 1 Parameters of Linear Fitting on FIX Protein Rebinding Assay

Sample	Intercept Value	Std. deviation, s	Slope, m	Correlation coefficient, R^2
polyDOP-μIDE-MIP	2.45E-08	3.89E-10	5.13E-09	0.97

Significant advances in this discipline have revealed the importance of π–π– stacking and π–cation interactions in the rational control of polyDOP self-assembly. Since the oxidation derivatives of DOP product readily adsorbs onto a metal electrode's surface, polymer passivation is irreversible. Figure 3a demonstrates this at the reduction peak between -0.02V and -0.08V. Although they are not prominent, this reduction peak can be attributed to the reductions of DAQ and DAC. The anodic peak at 1.2 V can be attributed to LDAC oxidation. Observations indicate that these peaks subside with each potential cycle. This suggests that the electrochemical pathway is functioning correctly. The polyDOP deposition is further demonstrated by the current response plot against time in Figure 3b. During the formation of a polyDOP passivating multilayer, the anodic and cathodic currents decreased, revealing the formation of the multilayer. This significant feature illustrates how the polyDOP layer covers the electrode as it thickens with each subsequent scan. A near-steady-state voltammogram is acquired after the tenth cycle. To produce polyDOP-IDE-MIP, a total of 13 potential cycles were executed.

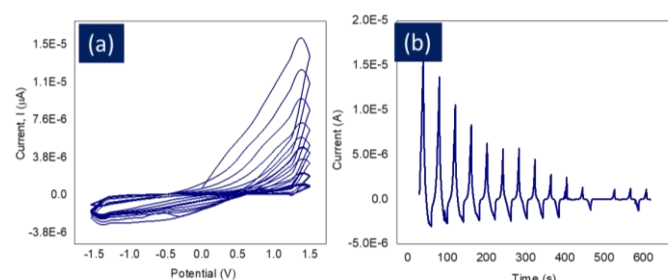

Figure 3. Molecular imprinting by electropolymerization. Cyclic voltammetry record of MIP development (a) and the current response over time plot (b).

3.3. FIX Protein Rebinding Assay

A potentiometric sensor measures the difference in potential between a working electrode and a reference electrode while operating with a current flow that is near to zero. Voltammetry is a subset of electro-analytical techniques that obtains information about an analyte by varying a potential and measuring the resulting current. Since there are numerous methods to alter a potential, there are also numerous types of voltammetry, such as linear sweep, differential pulse, square wave staircase, and more. In this case, linear sweep voltammetry was used by sweeping the voltage from -0.4 to 1.2 V. The scan rate is crucial because the duration of a scan must allow for a relevant chemical reaction to occur. According to Jolly and team (2016), 20 mV/s is required for DOP polymerization [19]. Thus, the present investigation maintained the same scan rate throughout analysis. Figure 4a shows a linear relationship between the concentration of FIX and the decrease in peak current. With polyDOP-μIDE-MIP alone, a prominent peak current of 2.87E-08 A at 0.3 V was observed. After each addition of FIX protein dilutions, the peak current gradually decreases. The peak current changes at 0.3 V have been normalized using equation 1, where I_i is the current response at the analyte concentration and I_o is the current response of bare polyDOP-μIDE-MIP.

$$\Delta I = I_i - I_o \tag{1}$$

The rebinding assay plot depicted in Figure 4b illustrates the mean value derived from three separate assessments, serving as evidence of the reproducibility of the measurements. In this relationship, the curve exhibits linear regions with the equations I_i= 2.23E-09ln($FIX_{concentration}$) + 2.45E-08. The calculation of the detection limit (LOD) involved adopting the formula 3.3*(s/m), where s represents the standard deviation of the intercept of the lowest concentration and m denotes the slope of the regression line. The LOD for FIX was determined to be 0.250 picomolar (pM). Table 1 presents the values obtained from the linear regression analysis.

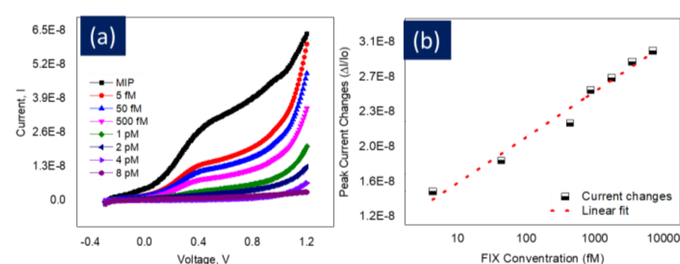

Figure 4. FIX protein rebinding assay. (a) The rebinding of FIX protein was monitored by linear-sweep voltammetry from -0.4 V to 1.2 V at 0.02 mV/s scan rate. (b) The peak current difference is plotted to determine the limit detection and the sensor's sensitivity.

Furthermore, the polydopamine-based molecularly imprinted polymer (polyDOP-μIDE-MIP) sensor offers notable benefits for the detection of FIX protein owing to its simple and cost-effective fabrication process. In the present work, the use of electrodeposited polyDOP demonstrates an improved and enhanced detection limit relative to our prior investigation by Letchumanan et al. (2019) [20]. The sensitivity of the developed sensor was determined by employing equation 2, yielding a value of 2.613E-10 A.fM^{-1}.μm^{-2}. Carbon has been shown to be an exceptional supporting material due to its favourable mechanical properties and strong compatibility with biomaterials . The act of combining GNU with carbon substance enhances charge transfer rate and increases the specific surface area. Thus, the sensor sensitivity at the nanoampere range may be attributed to the carbon and gold nanomaterial integration into the system.

$$Sensitivity = \frac{Slope\ of\ rebinding\ assay, m\ (A.fM^{-1})}{Active\ surface\ area, (\mu m^2)} \quad (2)$$

4. CONCLUSION

A polyDOP-µIDE-MIP sensor was efficiently produced employing an electropolymerization technique on a spiral-µIDE with a gap and electrode width of 50 µm. The polyDOP-µIDE-MIP sensor exhibits a detection limit of 0.250 pM when measuring pure FIX concentrations. Thus, the current study proved FIX protein detection is feasible using molecular-imprinting on a micro-gapped spiral IDE. Additionally, the research showcased the benefits of combining carbon and gold nanoparticles in order to enhance the sensitivity of the sensor.

REFERENCES

[1] J. Yao *et al.*, "Aptamer-antibody dual probes on single-walled carbon nanotube bridged dielectrode: Comparative analysis on human blood clotting factor," *Int. J. Biol. Macromol.*, vol. 151, pp. 1133–1138, 2020.

[2] H. Krishnan and S. C. B. Gopinath, "A potent anticoagulant hybrid of snake venom derived FIX-binding protein and anti-factor IX RNA aptamer: Assessed by in-silico and electrochemical analyses," *Int. J. Biol. Macromol.*, vol. 247, no. July, p. 125740, 2023.

[3] A. K. M. Shafiqul Islam, H. Krishnan, H. Singh, and M. N. Ahmad, "A noble molecular imprint polymer biosensor for caffeic acid detection in orthosiphon Stamineus extracts," *J. Teknol.*, vol. 77, no. 7, 2015.

[4] Archana *et al.*, "Electrochemical sensor based on polydopamine-molecularly imprinted polymer for detection of 4-ethylphenyl sulfate 'a novel gut metabolite': Fabrication, characterization, and performance evaluation in human urine," *Microchem. J.*, vol. 193, p. 108964, 2023.

[5] S. Li, S. Cao, M. J. Whitcombe, and S. A. Piletsky, "Size matters: Challenges in imprinting macromolecules," *Prog. Polym. Sci.*, vol. 39, no. 1, pp. 145–163, 2014.

[6] M. Mabrouk, S. F. Hammad, A. A. Abdella, and F. R. Mansour, "Tips and tricks for successful preparation of molecularly imprinted polymers for analytical applications: A critical review," *Microchem. J.*, vol. 193, p. 109152, 2023.

[7] X. Xie *et al.*, "Intervention of Polydopamine Assembly and Adhesion on Nanoscale Interfaces: State-of-the-Art Designs and Biomedical Applications," *Adv. Healthc. Mater.*, vol. 10, no. 9, p. 2002138, May 2021.

[8] S. Liu *et al.*, "Graphene oxide based molecularly imprinted polymers with double recognition abilities: The combination of covalent boronic acid and traditional non-covalent monomers," *Chem. Eng. J.*, vol. 290, pp. 220–231, 2016.

[9] R. Mirzajani and E. Arefiyan, "Construction and evaluation of a graphene oxide functionalized aminopropyltriethoxy silane surface molecularly imprinted polymer potentiometric sensor for dipyridamole detection in urine and pharmaceutical samples," *J. Braz. Chem. Soc.*, vol. 30, no. 9, pp. 1874–1886, 2019.

[10] F. Shahdost-fard and M. Roushani, "Impedimetric detection of trinitrotoluene by using a glassy carbon electrode modified with a gold nanoparticle@fullerene composite and an aptamer-imprinted polydopamine," *Microchim. Acta*, vol. 184, no. 10, pp. 3997–4006, 2017.

[11] H. Krishnan, S. C. B. Gopinath, M. K. M. Arshad, H. I. Zulhaimi, P. Anbu, and S. Subramaniam, "Molecularly imprinted polymer enhances affinity and stability over conventional aptasensor for blood clotting biomarker detection on regimented carbon nanohorn and gold nanourchin hybrid layers," *Sensors Actuators B Chem.*, vol. 363, no. December 2021, p. 131842, 2022.

[12] S. K. Arya, P. Zhurauski, P. Jolly, M. R. Batistuti, M. Mulato, and P. Estrela, "Capacitive aptasensor based on interdigitated electrode for breast cancer detection in undiluted human serum," *Biosens. Bioelectron.*, vol. 102, no. November 2017, pp. 106–112, 2018.

[13] C. P. Kurup, N. F. Mohd-Naim, C. Tlili, and M. U. Ahmed, "A Highly Sensitive Label-free Aptasensor Based on Gold Nanourchins and Carbon Nanohorns for the Detection of Lipocalin-2 (LCN-2).," *Anal. Sci. Int. J. Japan Soc. Anal. Chem.*, vol. 37, no. 6, pp. 825–831, Jun. 2021.

[14] H. Krishnan, S. C. B. Gopinath, M. K. Md. Arshad, H. Ii. Zulhaimi, and S. Ramanathan, "Molecularly imprinted polymer amalgamation on narrow-gapped Archimedean-spiral interdigitated electrodes: resistance to electrolyte fouling in acidic medium," *Microchim. Acta*, vol. 188, no. 4, p. 144, 2021.

[15] H. Krishnan, S. C. B. Gopinath, H. I. Zulhaimi, M. K. Md Arshad, and S. Subramaniam, "In silico structural analysis of truncated 2' fluoro-RNA aptamer: Elucidating EGF-1 and EGF-2 binding domains on factor IX protein," *Process Biochem.*, vol. 111, pp. 124–131, 2021.

[16] P. Palladino, M. Minunni, and S. Scarano, "Cardiac Troponin T capture and detection in real-time via epitope-imprinted polymer and optical biosensing," *Biosens. Bioelectron.*, vol. 106, pp. 93–98, 2018.

[17] G. Loget, J. B. Wood, K. Cho, A. R. Halpern, and R. M. Corn, "Electrodeposition of polydopamine thin films for DNA patterning and microarrays," *Anal. Chem.*, vol. 85, no. 21, pp. 9991–9995, 2013.

[18] W. Yu, X. Lin, N. Duan, Z. Wang, and S. Wu, "A fluorescence and surface-enhanced Raman scattering dual-mode aptasensor for sensitive detection of deoxynivalenol based on gold nanoclusters and silver nanoparticles modified metal-polydopamine framework," *Anal. Chim. Acta*, vol. 1244, p. 340846, 2023.

[19] P. Jolly, V. Tamboli, R. L. Harniman, P. Estrela, C. J. Allender, and J. L. Bowen, "Aptamer-MIP hybrid receptor for highly sensitive electrochemical detection of prostate specific antigen," *Biosens. Bioelectron.*, vol. 75, pp. 188–195, 2016.

[20] I. Letchumanan, S. C. B. Gopinath, M. K. Md Arshad, P. Anbu, and T. Lakshmipriya, "Gold nano-urchin integrated label-free amperometric aptasensing

human blood clotting factor IX: A prognosticative approach for 'Royal disease,'" *Biosens. Bioelectron.*, vol. 131, no. January, pp. 128–135, 2019.